

Steady-State Traveling Waves on the Surface of a Viscous Liquid Film Falling Down on Vertical Wires and Tubes

Yu. Ya. Trifonov

Institute of Thermophysics, Siberian Branch, USSR Academy of Sciences, Novosibirsk, USSR

Various nonlinear wavy regimes of a viscous liquid film flowing down vertical wires and tubes were calculated using the integral method. The linear stability analysis of the trivial smooth solution was compared with the results published previously. In the region of linear instability, the competition among the gravity, viscous and capillary forces formed the steady-state traveling solutions of finite amplitudes. At least two families of waves were shown to be parameterized by the wave number for given values of external parameters (Reynolds number, cylinder radius and physical characteristics of liquid). The basic waves characteristics depended on external parameters and on wave number. The intensity of wavy processes increased with decreasing cylinder radius. The calculations show the catastrophic growth of wave amplitude, when the system flows down a vertical tube of sufficiently small radius and moves into the linear, unstable region.

Introduction

Many experimental and theoretical works have been performed on the wavy hydrodynamics of a viscous film falling down the vertical plane. In their experiments, Kapitza and Kapitza (1949) and Alekseenko et al. (1985) used a cylinder with radius greater than the film thickness, instead of a vertical plane. Kapitza and Kapitza (1949) carried out the experiments on a short vertical section of a glass cylinder (250 mm long and 35 mm in dia.). The film of water or alcohol fell down the outer surface of cylinder. To regulate the wave regimes of flow, pulsations of the flow rate were introduced. The wave amplitudes, phase velocities, lengths of waves, thicknesses of films were measured. The observed regular steady-state traveling waves were classified by the authors as "periodical" and "single." The experimental results were given only for a periodical regime at $Re = 5-20$.

Alekseenko et al. (1985) obtained more comprehensive and complete experimental results. To regulate wave formation, pulsation of the flow rate was introduced on the input section too. The wave profile was similar to a sine function if the frequency of pulsation was high and became more nonlinear (abrupt front of wave and flowing back of wave) if the frequency was low. They presented results for both types of the observed waves.

In other experiments, the hydrodynamics of a wavy film

flowing down wires and tubes with radii comparable with the film thickness were investigated. Goren (1962) studied both theoretically and experimentally the instability of an annular thread of fluid creeping into the wall of a thin wire or tube. In Goren's theory and experiment, wires or tubes with an extremely small radius were considered such that gravitational forces could be negligible in comparison with the viscous and surface forces.

In the present study, we consider all possible forces in a flowing film, and the experiments discussed above are special cases in the limit when the wall curvature is zero or large.

Benjamin (1957) and Yih (1963), using an analytical approximation of Orr-Zommerfeld's equation, have found that falling film down a vertical plane with a smooth free surface is unstable with respect to long-wave disturbances at any flow rates. Similar results for the case of the falling down of a vertical cylinder were obtained by Lin and Liu (1975) and Tougou (1977). In a neighborhood of the neutral curve, nonlinear periodical solutions were considered by Lin (1969), Benney (1966), Nakaya (1975), Gjevik (1970), and Nepomnyashchy (1974) for the case of the falling down of a vertical plane. Tougou (1977) and Shlang and Sivashinsky (1982) derived the nonlinear asymptotic equation for the surface elevation when the liquid film falling down a vertical cylinder with a small

wall curvature was considered. In the neighborhood of neutral curve, Tougou (1977) obtained the waves of finite amplitudes. Shlang and Sivashinsky (1982) considered the linear stability of smooth flow with respect to two-dimensional disturbances of the film free surface and found that for small values of cylinder radii, a wavy flow was a one-dimensional train of rings.

The latest important progress on the theory of nonlinear waves on the surface of the falling down of a vertical plane liquid film was achieved by Trifonov and Tselodub (1985, 1988, 1991) and Demekhin and Shkadov (1985). They used a model system of equations obtained from an integral method. The various steady, traveling, periodical, nonlinear wave regimes were obtained for this system. It was shown that there were a great number of the waves families parameterized by the wave number. The linear stability of nonlinear solutions with respect to all possible disturbances was investigated, and a bifurcation analysis was carried out. It was shown that two types of waves were distinguished. The comparison with the experimental results demonstrated good quantitative agreement.

The aim of this work is to generalize the methods and results presented by Trifonov and Tselodub (1991) and to investigate the nonlinear waves on the surface of a liquid film falling down a vertical wire or tube.

Governing Equations

We considered a two-dimensional flow of a viscous incompressible liquid down the outer and the inner walls of a circular cylinder, as shown in Figures 1a and 1b. Using the usual dimensionless variables, the governing equations of the fluid motion and the boundary conditions are as follows:

$$\epsilon^2 \left(\frac{\partial v^*}{\partial t^*} + v^* \frac{\partial v^*}{\partial r^*} + u^* \frac{\partial v^*}{\partial z^*} \right) = -\frac{\partial P^*}{\partial r^*} + \frac{\epsilon}{Re_1} \left(\epsilon^2 \frac{\partial^2 v^*}{\partial z^{*2}} + \frac{\partial^2 v^*}{\partial r^{*2}} + \frac{1}{r^*} \frac{\partial v^*}{\partial r^*} - \frac{v^*}{r^{*2}} \right)$$

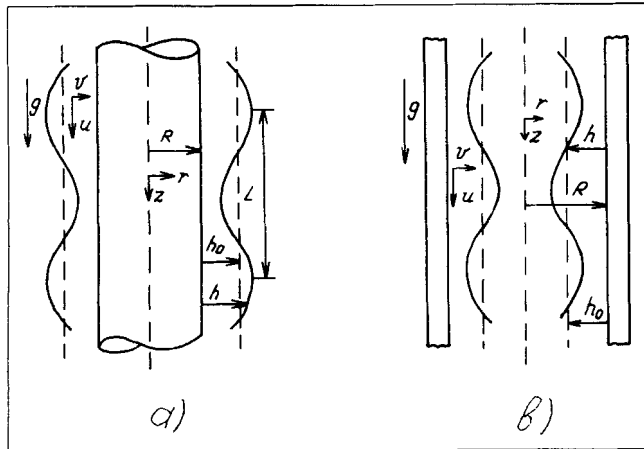


Figure 1. The flow.

- Film falling down on the outer wall of a circular cylinder: case of wire.
- Film falling down on the inner wall of a circular cylinder: case of tube.

$$\begin{aligned} \frac{\partial u^*}{\partial t^*} + v^* \frac{\partial u^*}{\partial r^*} + u^* \frac{\partial u^*}{\partial z^*} &= -\frac{\partial P^*}{\partial z^*} + \frac{\epsilon}{Re_1} \frac{\partial^2 u^*}{\partial z^{*2}} \\ &+ \frac{1}{\epsilon Re_1} \left(\frac{\partial^2 u^*}{\partial r^{*2}} + \frac{1}{r^*} \frac{\partial u^*}{\partial r^*} + 3 \right) \\ \frac{\partial(u^* r^*)}{\partial z^*} + \frac{\partial(v^* r^*)}{\partial r^*} &= 0 \\ u^* = v^* &= 0, \quad r^* = R^* \\ P^* &= P_o^* + \frac{2\epsilon}{Re_1} \frac{\frac{\partial v^*}{\partial r^*} - \epsilon^2 \left(\frac{\partial h^*}{\partial z^*} \right)^2 \frac{\partial u^*}{\partial z^*}}{1 - \epsilon^2 \left(\frac{\partial h^*}{\partial z^*} \right)^2} - \frac{3^{1/3} Fi^{1/3} \epsilon^2}{Re_1^{5/3}} \\ &\times \left\{ \frac{\frac{\partial^2 h^*}{\partial z^{*2}}}{\left[1 + \epsilon^2 \left(\frac{\partial h^*}{\partial z^*} \right)^2 \right]^{3/2}} \mp \frac{1}{\epsilon^2 r^* \left[1 + \epsilon^2 \left(\frac{\partial h^*}{\partial z^*} \right)^2 \right]^{3/2}} \right\}, \\ r^* &= R^* \pm h^*(z^*, t^*) \\ \frac{\partial u^*}{\partial r^*} + \epsilon^2 \frac{\partial v^*}{\partial z^*} + \frac{2\epsilon^2 \frac{\partial h^*}{\partial z^*}}{1 - \epsilon^2 \left(\frac{\partial h^*}{\partial z^*} \right)^2} \cdot \left(\frac{\partial v^*}{\partial r^*} - \frac{\partial u^*}{\partial z^*} \right) &= 0, \\ r^* &= R^* \pm h^*(z^*, t^*) \quad (1) \end{aligned}$$

where $u^* = u/u_o$, $v^* = (v/u_o)L/h_o$, $x^* = x/L$, $r^* = r/h_o$, $t^* = tu_o/L$, $P^* = P/\rho u_o^2$, $\epsilon = h_o/L$, $Re_1 = u_o h_o/\nu$, $Fi = (\sigma/\rho)^3/g\nu^4$, $u_o = gh_o^2/3\nu$, Fi is the film number, u is the velocity in the z -direction, v is the velocity in the r -direction, P is the pressure, P_o^* is the atmospheric pressure, g is the acceleration due to gravity, ν is the kinematic viscosity, ρ is the density, σ is the coefficient of surface tension, and h is the instantaneous thickness of the film. The upper or lower sign, "+" or "-" in the above and subsequent equations, refers to the case of wire or tube, respectively (that is, the flowing of film on outer or inner wall of a circular cylinder).

It is appropriate here to use some scale related to the wave length L as a characteristic scale of length in the z -direction, the mean film thickness h_o as that in the r -direction, and the mean velocity u_o of a smooth flowing on vertical plane as a velocity scale.

We shall consider only long-wave disturbances, therefore, $\epsilon \ll 1$. For the range of Reynolds numbers under consideration $\epsilon \ll Re \leq 1/\epsilon$ after neglecting terms smaller than $O(\epsilon)$, the system of Eq. 1 is simplified substantially. In the dimension form, it is as follows:

$$\begin{aligned} \frac{\partial u}{\partial t} + v \frac{\partial u}{\partial r} + u \frac{\partial u}{\partial z} &= -\frac{1}{\rho} \frac{\partial P}{\partial z} + g + \nu \cdot \left(\frac{\partial^2 u}{\partial r^2} + \frac{1}{r} \frac{\partial u}{\partial r} \right) \\ \frac{\partial P}{\partial r} &= 0 \end{aligned}$$

$$\frac{\partial(ur)}{\partial z} + \frac{\partial(vr)}{\partial r} = 0$$

$$u = v = 0, \quad r = R; \quad \frac{\partial u}{\partial r} = 0, \quad r = R \pm h(z, t)$$

$$P = P_o - \sigma \cdot \left(\mp \frac{1}{R \pm h} + \frac{\partial^2 h}{\partial z^2} \right) \quad (2)$$

In addition, the following kinematic condition on the free surface must be satisfied:

$$\pm v = \frac{\partial h}{\partial t} + u \frac{\partial h}{\partial z}, \quad r = R \pm h(z, t)$$

In deriving Eqs. 2 from Eqs. 1, we retain the term with the capillary pressure in boundary condition. This is true if the film number $Fi \sim Re^5/\epsilon^6$, which holds in most experiments.

It is easy to see that one solution of Eqs. 2 is:

$$u = \frac{gR^2}{4\nu} \left[1 - \left(\frac{r}{R} \right)^2 + 2 \left(1 \pm \frac{h_o}{R} \right)^2 \cdot \ln \frac{r}{R} \right]$$

$$v = 0, \quad P = P_o - \sigma \left(\mp \frac{1}{R \pm h_o} \right), \quad h = h_o = \text{const}$$

This solution is related to smooth flow and exists for any liquid flow rate.

Other solutions of Eqs. 2 are difficult to arrive at. To simplify this problem, it is convenient to use the following assumption on the velocity profile:

$$u(r, z, t) = \pm \frac{q(z, t)}{Rf_{\pm}[h(z, t)/R]} \times \left[1 - \left(\frac{r}{R} \right)^2 + 2 \left(1 \pm \frac{h(z, t)}{R} \right)^2 \cdot \ln \frac{r}{R} \right]$$

$$q(z, t) = \pm \frac{1}{R} \cdot \int_R^{R \pm h} u r dr$$

$$f_{\pm}(h/R) = \frac{1}{4} - (1 \pm h/R)^2 + (1 \pm h/R)^4 \times \left(\frac{3}{4} - \ln(1 \pm h/R) \right) \quad (3)$$

This profile satisfies the no-slip condition at the solid-fluid interface $r = R$ and the condition of vanishing net force at each element of the fluid-air interface $r = R \pm h(z, t)$. For the case of smooth flow, the profile gives us the exact solution of Navier-Stokes equations.

In the limit $R \rightarrow \infty$ (the flowing of viscous fluid down the vertical plane), this profile offers:

$$u(\delta, z, t) = \frac{3q(z, t)}{h(z, t)} \cdot \left(\frac{\delta}{h(z, t)} - \frac{\delta^2}{2h^2(z, t)} \right)$$

where δ is the distance from the wall.

For this case, where some experimental results and direct numerical simulations use the Navier-Stokes equations, this assumption is valid for the values of Reynolds numbers under consideration. Thus, Nakoryakov et al. (1977) experimentally

demonstrated that the velocity profile was close to a semiparabolic one for the greater part of the wavy film flow. Similar results were obtained by Bach and Villadsen (1984), who solved the nonstationary Navier-Stokes equations by using a finite-element scheme. Trifonov and Tsveldub (1988, 1991) demonstrated that the thickness profiles and other characteristics of nonlinear waves obtained by using this velocity profile assumption quantitatively corresponded to Alekseenko et al.'s (1985) experiments.

For long waves flowing down a circular cylinder, this assumption (Eqs. 3) is also reasonable. It is extremely difficult to evaluate the correctness of the assumption in Eqs. 3 mathematically. The physical correctness of relation 3 may be proved by comparing the solutions of the simplified system with experimental results and with the results obtained by using the Navier-Stokes equations.

Taking into account that the pressure in Eqs. 2 is the function of only z and t , we substitute the profile in Eqs. 3 into Eqs. 2, multiply the equation by r , and integrate over the r -direction from R to $R \pm h(z, t)$:

$$\pm \frac{\partial q}{\partial t} \pm 1.2 \frac{\partial}{\partial z} \left(\frac{q^2}{h} \cdot f_1 \left(\pm \frac{h}{R} \right) \right) = \left\{ g + \frac{\sigma}{\rho} \left[\frac{1}{(R \pm h)^2} \frac{\partial h}{\partial z} + \frac{\partial^3 h}{\partial z^3} \right] + \frac{3\nu q}{h^3 f(\pm h/R)} \right\} \cdot \left(\pm h + \frac{h^2}{2R} \right)$$

$$\frac{\partial h}{\partial t} + \frac{R}{R \pm h} \frac{\partial q}{\partial z} = 0$$

$$f = 3 \left\{ \frac{1}{4} - y^2 + y^4 \cdot \left[\frac{3}{4} - \ln(y) \right] \right\} / 4(y-1)^3 \quad y = 1 \pm h/R$$

$$f_1 = (y-1) \cdot \left[-\frac{1}{6} + \frac{5}{4} \cdot y^2 - \frac{5}{2} \cdot y^4 + \frac{17}{12} \cdot y^6 + 2y^4 \ln(y) - 3y^6 \ln(y) + 2y^6 \ln^2(y) \right] / \left\{ 1.2 \cdot \left[\frac{1}{4} - y^2 + y^4 \cdot \left(\frac{3}{4} - \ln(y) \right) \right]^2 \right\} \quad (4)$$

To derive the system of Eqs. 4, we used the kinematic condition presented above. In the limit $R \rightarrow \infty$ ($f_1 \rightarrow 1$, $f \rightarrow 1$), this system is from Shkadov's (1967).

We mark here that the analogous integral method was used by Demekhin et al. (1988) to investigate the nonlinear waves on the surface of a magnetic liquid falling down the outer surface of a vertical cylinder. Without magnetic field, their system of equations corresponds to the particular case of Eqs. 4. It differs from the equations obtained by Demekhin et al. (1988). The system of Eqs. 4 is valid both for the fall-down of the outer and inner surfaces of vertical cylinder and the correctness criteria $\epsilon \ll 1$, $\epsilon \ll Re \leq 1/\epsilon$, $Fi \sim Re^5/\epsilon^6$ of assumptions used here.

In this work, the wave regimes of flowing film will be studied on the basis of Eqs. 4. It differs from the nonlinear asymptotic equations of Tougou (1977), Lin and Liu (1975), Shlang and Sivashinsky (1982). The system of Eqs. 4 is valid for a wide range of the wall curvature and for describing an evolution of disturbances with large amplitudes.

The solution of Eqs. 4 related to the smooth flow is:

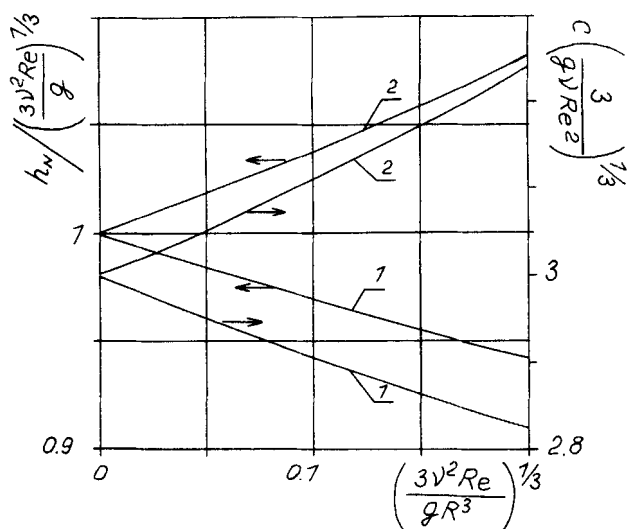


Figure 2. Values of the smooth solution thickness and the neutral disturbance phase velocity.

Line 1, film flowing down on a wire; line 2, on a tube.

$$h = h_N, \quad q = q_N = -\frac{gh_N^3}{3\nu} \cdot f(y_N), \quad y_N = 1 \pm h_N/R$$

In the flow-down of a vertical plane, Nusselt's solution is well known. To investigate its stability with respect to infinitesimal disturbances:

$$h = h_N + h', \quad q = q_N + q', \quad (h', q') \sim \exp[i\alpha(z - ct)]$$

where $\alpha = 2\pi/\lambda$, λ = disturbance period. The system of Eqs. 4 is linearized with respect to h' and q' , and it is not difficult now to resolve the condition:

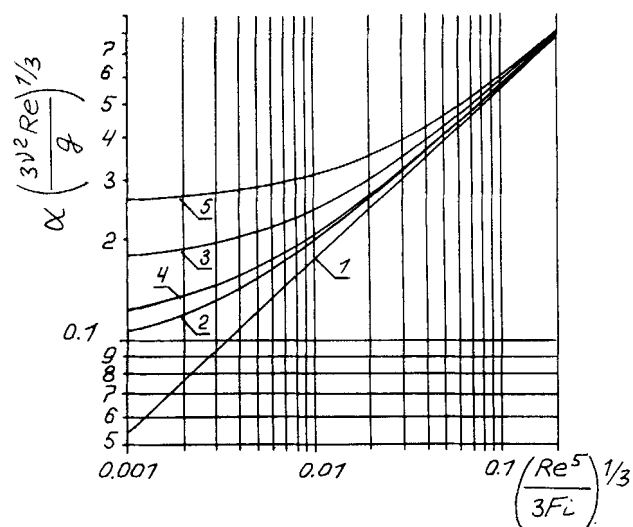


Figure 3. Stability curves for various cylinder radius.

Lines 1-3, case of wire with $R^{*-1} = 0, 0.1$ and 0.2 , respectively; lines 4, 5, tube with $R^{*-1} = 0.1, 0.2$. Disturbances with the wave numbers situated below stability curves are unstable.

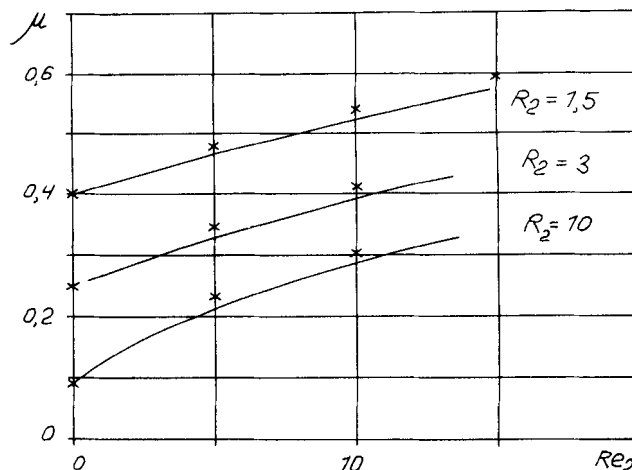


Figure 4. Stability curves: this study, solid lines, Lin and Liu (1975) theory, asterisks, for various values of the wire radius at $We_2 = 100$.

$$\begin{aligned} & -c^2 y_N \\ & + c \left(2.4 \frac{q_N}{h_N} y_N f_1(y_N) \mp \frac{3\nu y_N R (y_N^2 - 1)}{2i\alpha h_N^3 f(y_N)} \right) \pm \frac{\sigma R (y_N^2 - 1)}{2\rho} \alpha^2 \\ & - \left(1.2 \frac{q_N^2}{h_N^2} f_1(y_N) \mp 1.2 \frac{q_N^2}{h_N R} \frac{df_1}{dy} \bigg|_{y=y_N} \pm \frac{\sigma}{\rho R} \frac{y_N^2 - 1}{2y_N^2} \right) \\ & \pm \frac{3\nu q_N R (y_N^2 - 1)}{2i\alpha h_N^3 f^2(y_N)} \left(\frac{3f(y_N)}{h_N} \pm \frac{1}{R} \frac{df}{dy} \bigg|_{y=y_N} \right) = 0 \quad (5) \end{aligned}$$

Since temporal stability with respect to spatially periodic disturbances is of interest here, the wave number in Eq. 5 is assumed to be real. Then, the values of complex phase velocity c may be found from Eq. 5. If $Im(c) > 0$, the disturbance is amplified; if $Im(c) < 0$, it disappears.

Using the scales q_N and $h^* = (3\nu q_N/g)^{1/3}$ for the values of

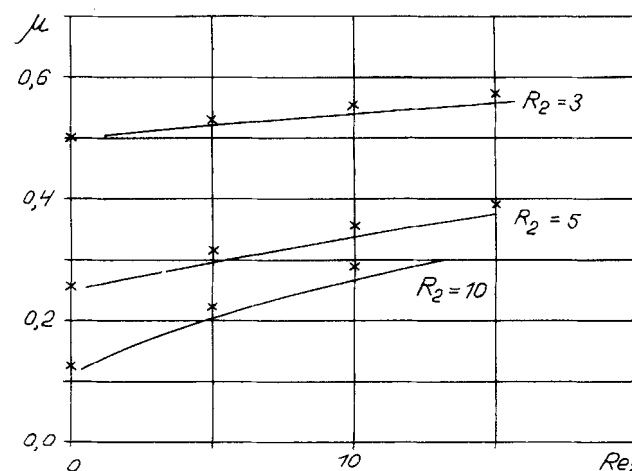


Figure 5. Stability curves: this study, solid lines, Lin and Liu (1975) theory, asterisks, for various values of the tube radius at $We_2 = 100$.

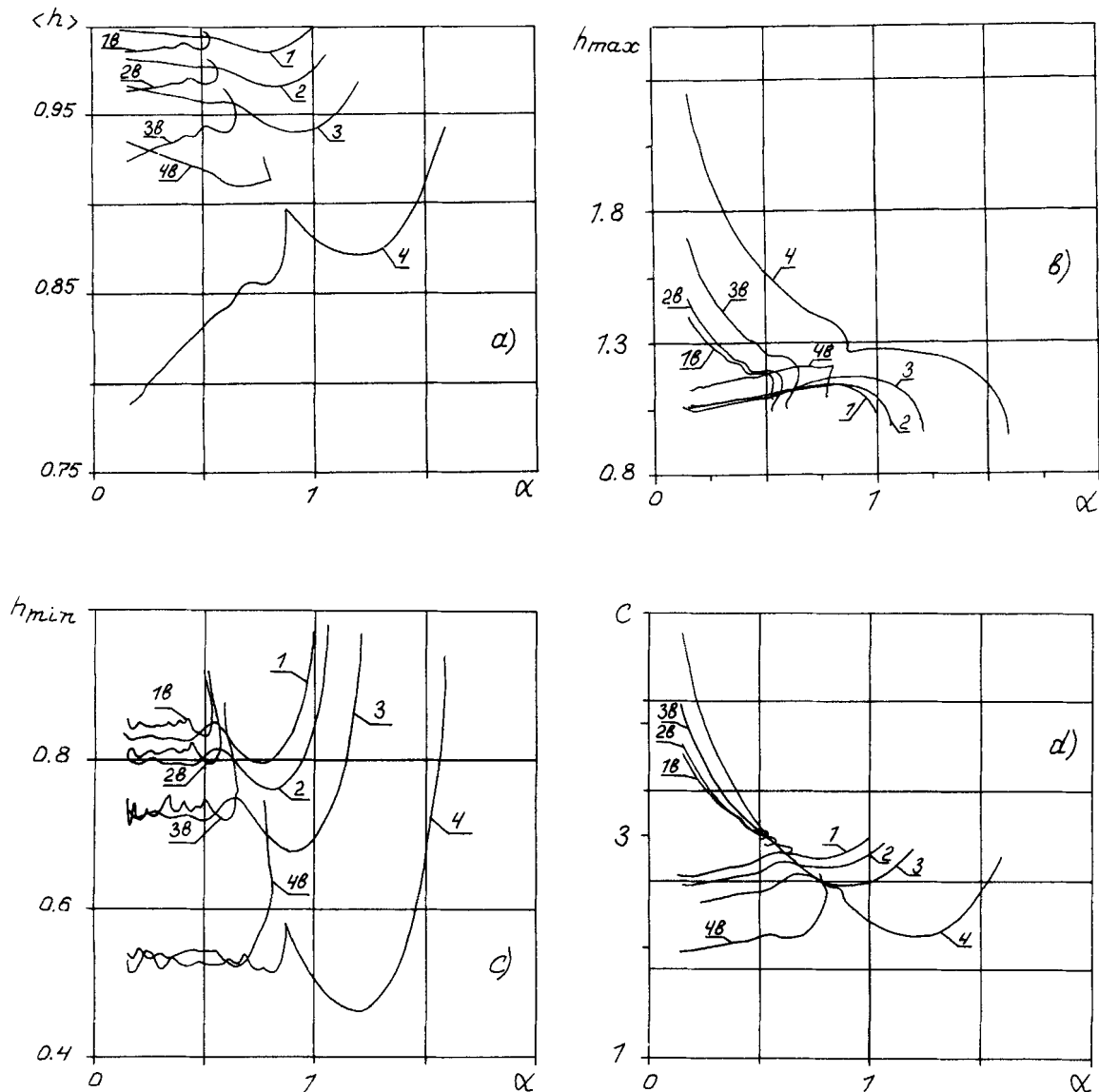


Figure 6. Characteristics of waves vs. wave number at $Re=4$, $Fi^{1/11}=6.8$.

Two branches of waves presented are: lines 1, 1b, wire with $R^{-1}=0$; lines 2, 2b, $R^{-1}=0.05$; lines 3, 3b, $R^{-1}=0.1$; lines 4, 4b, $R^{-1}=0.2$.

q_N , h_N , and R , respectively, we can obtain the neutral curve [$Im(c)=0$], the phase velocity of neutral disturbances, and the smooth solution in dimensionless form as follows:

$$(\alpha_{neut}^*)^2 = \pm \frac{2}{WeR^*(y_N^2-1)} \left(y_N c_{neut}^{*2} - 2.4 \frac{1}{h_N^*} \cdot y_N f_1 c_{neut}^* + 1.2 \frac{f_1}{h_N^{*2}} \mp \frac{1.2}{h_N^* R^*} \cdot \frac{df_1}{dy} \bigg|_{y=y_N} \pm We \cdot \frac{y_N^2-1}{2y_N^2 R^*} \right)$$

$$c_{neut}^* = \frac{1}{y_N f(y_N) h_N^*} \left(3f(y_N) \pm \frac{h_N^*}{R^*} \frac{df}{dy} \bigg|_{y=y_N} \right)$$

$$1 + h_N^{*3} f(y_N) = 0 \quad (6)$$

where $h_N^* = h_N/h^*$, $c^* = ch^*/q_N$, $R^* = R/h^*$, $We = (\sigma/\rho)h^*/q_N^2 = (3Fi/Re^5)^{1/3}$, $Re = q_N/\nu$, $Fi = (\sigma/\rho)^3/g\nu^4$, $\alpha^* = \alpha h^*$.

Disturbances with $\alpha^* < \alpha_{neut}^*$ are unstable [$Im(c^*) > 0$], and those with $\alpha^* > \alpha_{neut}^*$ disappear.

The value of the neutral disturbance phase velocity c_{neut}^* and that of the smooth solution thickness h_N^* depend only on the values of the dimensionless cylinder radius, as it follows from Eqs. 6 and are shown in Figure 2. Lines 1 and 2 correspond to the cases of wire and tube, respectively. With decreasing cylinder radius, the neutral disturbance phase velocity and the value h_N^* increase for the flow-down of the inner cylinder wall and decrease for that of the outer cylinder wall.

The dependence of the neutral disturbance wave number on the value of We^{-1} number for various cylinder radius is shown in Figure 3. Lines 1–3 correspond to the case of wire with $R^{-1}=0$, 0.1 and 0.2, respectively and lines 4 and 5 to the case of tube with $R^{-1}=0.1$ and 0.2.

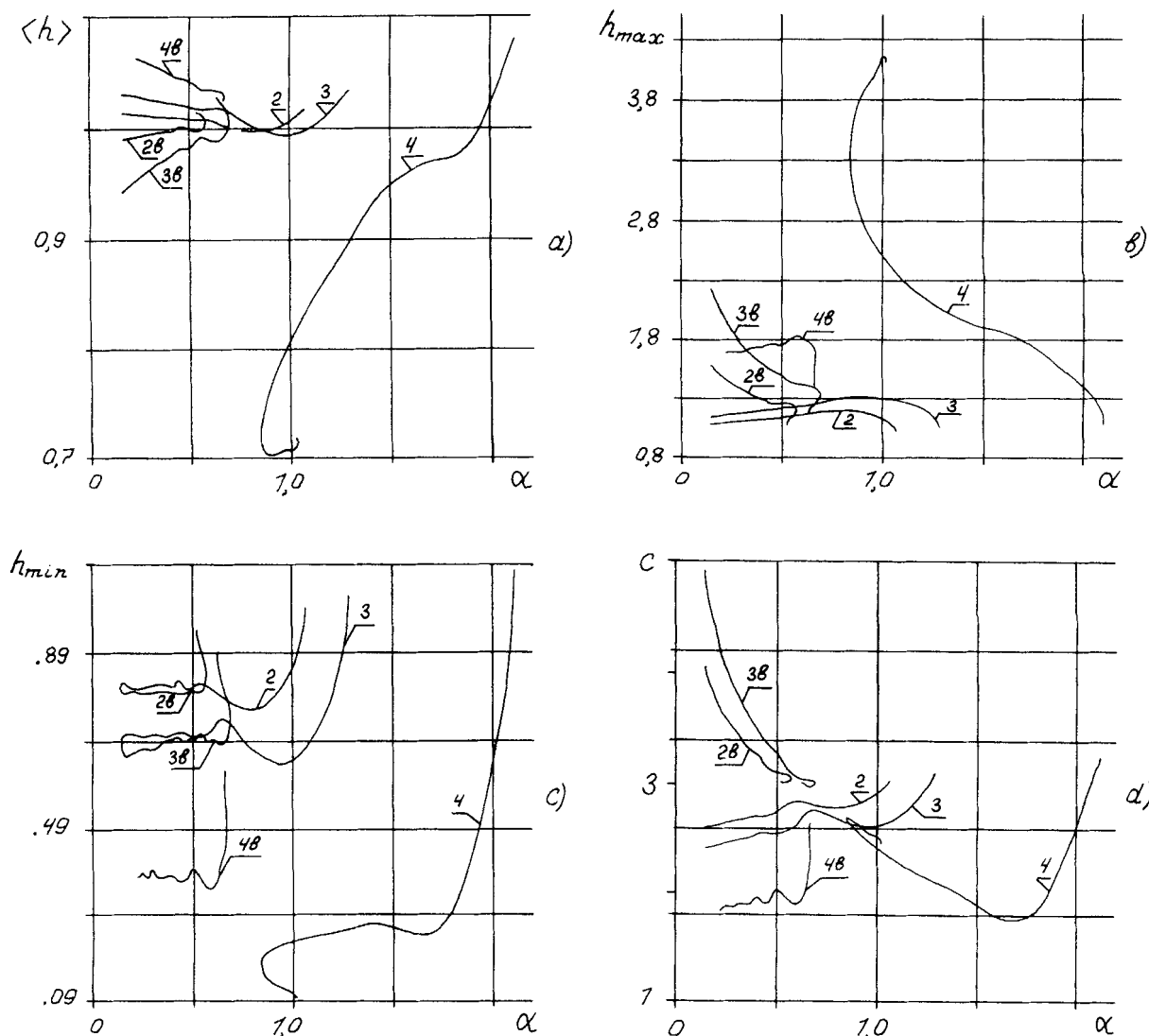


Figure 7. Characteristics of waves vs. wave number at $Re=4$, $Fi^{1/11}=6.8$.

Two branches of waves presented are: lines 2, 2b, tube with $R^{-1}=0.05$; lines 3, 3b, $R^{-1}=0.1$; lines 4, 4b, $R^{-1}=0.2$.

Unlike the case of flow-down, the vertical plane ($R^{*-1}=0$) analyzed by Shkadov (1967) and Alekseenko et al. (1985), dependences on α_{neut}^* (We^{-1}) for $R^{*-1} \neq 0$ do not go to zero with decreasing Re .

It is possible now to estimate the limits of long-wave approximation. As a characteristic scale L in z -direction, introduced above, we may take the wavelength of neutral disturbance and it is easy to see that $\epsilon \approx \alpha_{\text{neut}}^*/2\pi$. As shown in Figure 3, the correlation $\epsilon \ll 1$ is fulfilled satisfactorily for the range of parameters $5 \leq R^* < \infty$, $4 \leq Fi^{1/11} \leq 10$, $0 \leq Re \leq 20$, considered here.

To evaluate the correctness of the assumption of Eqs. 3, our results on the smooth solution linear stability analysis are compared with Lin and Liu's (1975) theory, Figures 4-5.

To obtain the neutral curves, Lin and Liu (1975) used the Navier-Stokes equation and its expanded solution in power series of $\mu = 2\pi h_N/\lambda$. Reynolds number in Figures 4-5 $Re_2 = u_{\text{max}} h_N/\nu$, u_{max} is the velocity on the free film surface, $R_2 = R/h_N$, $c_2 = c/u_{\text{max}}$. Lin and Liu's (1975) results are shown by asterisks, which correspond to the case of film with $We_2 = \sigma/$

$(\rho g h_N^2) = 100$ flowing down the different wires (Figure 4) and tubes (Figure 5). Our results at the same value of We_2 and for the same values of the cylinder radius are presented by the solid lines. The comparison demonstrates satisfactory agreement.

To calculate the periodical steady-state traveling solutions of Eqs. 4, $q = q(z - ct)$, $h = h(z - ct)$ and c -phase velocity with the finite amplitude, the dimensionless form of these equations was used as follows:

$$-c^* \frac{dq^*}{d\xi^*} + 1.2 \frac{d}{d\xi^*} \left(\frac{q^{*2}}{h^*} \cdot f_1(y) \right) = \left\{ \pm We \left(\frac{1}{(R^* \pm h^*)^2} \frac{dh^*}{d\xi^*} + \frac{3}{We} \frac{d^3 h^*}{d\xi^{*3}} \right) + Z \left(\pm 1 \pm \frac{q^*}{h^{*3} f(y)} \right) \right\} \left(\pm h^* + \frac{h^{*2}}{2R^*} \right)$$

$$q^* = 1 \pm c^* \left(\pm h^* + \frac{h^*}{2R^*} - \left\langle \pm h^* + \frac{h^{*2}}{2R^*} \right\rangle \right), \quad y = 1 \pm \frac{h^*}{R^*} \quad (7)$$

where $\xi^* = \sqrt{3/We} \cdot \xi/h_s$, $\xi = z - ct$, $h^* = h/h_s$, $R^* = R/h_s$, $q^* = q/q_0$, $c^* = ch_s/q_0$, $h_s = (3\nu q_0/g)^{1/3}$, $We = (3Fi/Re^5)^{1/3}$, $Z = (81Fi/Re^{11})^{1/6}$, $Re = q_0/\nu$, $q_0 = \langle q \rangle = (1/\lambda) \int_0^\lambda q(\xi) d\xi$, and λ is the wavelength of solution.

Eliminating the flow rate $q(\xi)$ (asterisk is omitted from now on) from the first equation of Eqs. 7, we yield one equation to calculate $h(\xi)$ and phase velocity c . The periodical wave with wave number α is presented as a Fourier series:

$$h(\xi) = \sum_{-\infty}^{\infty} H_n \exp[i\alpha n \xi], \quad \overline{H}_{-n} = H_n \quad (8)$$

Overbar denotes the operation of complex conjugation.

Taking into account the first $N/2$ harmonics in the set of Eqs. 8, and substituting it into another equation we obtain a system of $N+1$ equations for the real unknowns H_0 , c and $N/2$ complex ($H_1, \dots, H_{N/2}$). The pseudo-spectral method and the fast Fourier transformation procedure were used to calculate the harmonics of nonlinear terms.

Since Eqs. 7 are invariant to the shifts $\xi^* \rightarrow \xi^* + \text{const}$, the origin of coordinates was usually chosen such that $\text{Im} \text{age}(H_1) = 0$.

Thus, the system of algebraic equations is completed, and Newton-Kantorovich's method was used to solve it numerically. To reduce the number of harmonics in the set of Eqs. 8, the following convergence criterion was taken:

$$|H_{N/2}| / \sup |H_n| < 10^{-3}$$

For this purpose, the number N had to be varied depending on the values α and Re , Fi over the range from 16 to 128.

We gave here only the scope of the numerical method. The procedure in more details was presented by Trifonov and Tsveldub (1991), where nonlinear waves on the surface of film falling down a vertical plane were considered.

Steady-State Traveling Wave Calculations

The calculations were based on Eqs. 7. We used three ex-

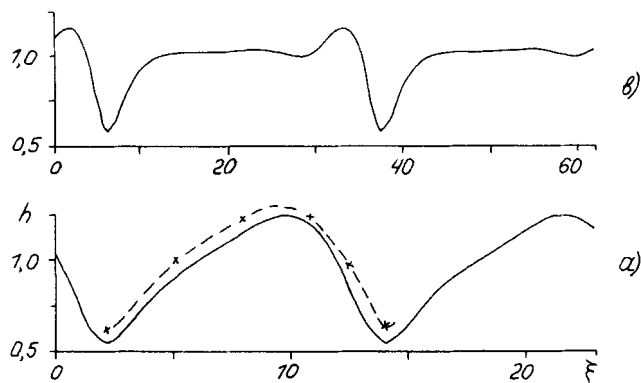


Figure 8. Characteristics of the first-family waves for the case of falling down on a vertical plane.

The dashed line is the corresponding experimental profile, where $Re = 7.2$, $Fi^{1/11} = 4.87$, $\alpha \approx 0.532$ (profile a), $\alpha \approx 0.2$ (profile b).

ternal parameters, R , Z , and We or R , Fi , and Re , and one internal parameter, α —wave number. External parameters have a clear physical sense. To understand the meaning of internal parameter, α , it is necessary to discuss some experimental results. In the experiments of Kapitza and Kapitza (1949) and Alekseenko et al. (1985) the free film surface, without artificial perturbation, was covered with irregular waves, and the wavy structure was extremely sensitive to external disturbances. If external periodical impulses in time were introduced at the input section of the liquid flow, regular waves in space, which travel steadily in term, were formed. The wavelength was conditioned by the impulse frequency, but the wave amplitude did not depend on the amplitude of the external disturbance. Thus, by varying the disturbance frequency, various wave regimes were observed for a given flow rate. Kapitza divided the waves into two classes: "periodical" and "solitary" waves.

The main difficulty in finding the solutions of Eqs. 7 by Newton's method is to determine the initial approximation that is close enough to the solution. The periodical steady-state traveling solutions with wave numbers close to neutral ones for the fall-down on the vertical plane were first obtained analytically by Shkadov (1967). Using this result as an initial approximation and employing a small enough step on the parameters, α , R , Fi , and Re , in the region of linear instability, the steady-state solutions were found for a wide range of external parameters and up to the smallest values of α considered here. Results are presented in Figures 6–16. As there are many parameters, a detailed investigation is very difficult to carry out, and the main concern is with the qualitative difference of

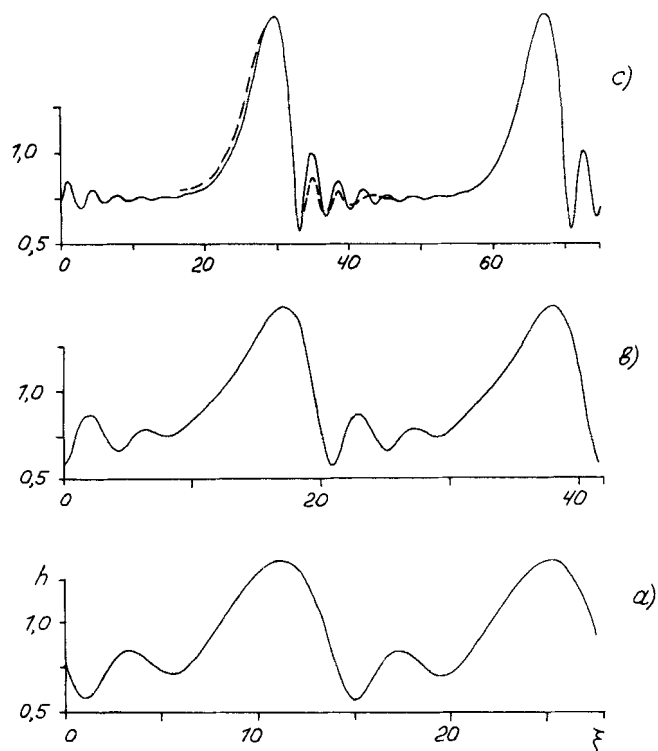


Figure 9. Characteristics of the second-family waves for the case of falling down on a vertical plane.

The dashed line is the corresponding experimental profile, where $Re = 7.2$, $Fi^{1/11} = 4.87$, $\alpha = 0.45$ (profile a), $\alpha = 0.3$ (profile b), and $\alpha \approx 0.167$ (profile c).

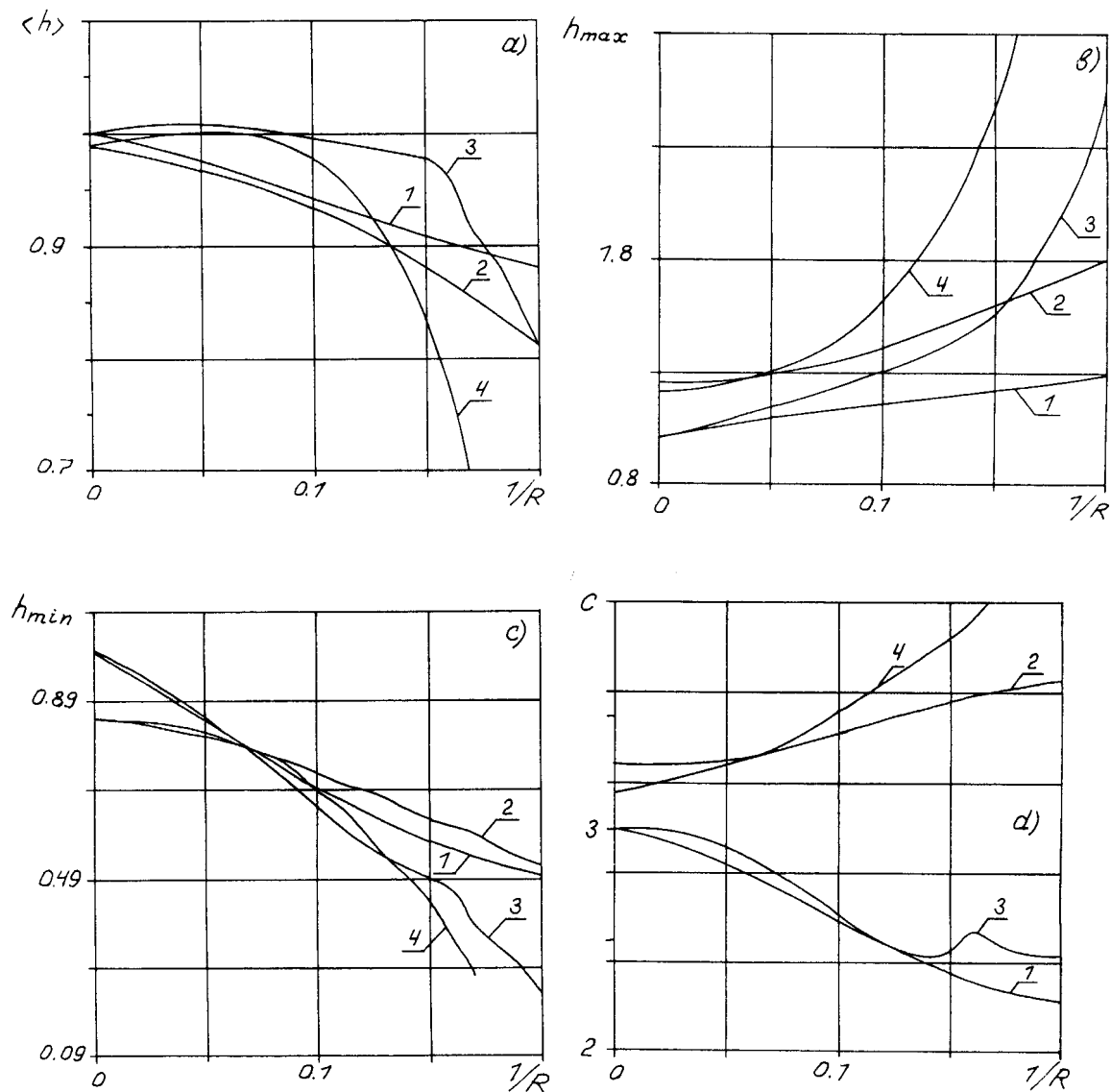


Figure 10. Characteristics of waves vs. wall curvature at $Re=4$, $Fi^{1/11}=6.8$.

Lines 1, 2, case of wire; lines 3, 4, tube; lines 1, 3, wave with $\alpha=1.0$ branched from the trivial solution; line 2, $\alpha=0.32$ (long wave); line 4, $\alpha=0.4$ (long wave).

waves falling down on the inner or outer cylinder to those falling down on a vertical plane.

Figures 6 and 7 show the dependence of the dimensionless basic wave characteristics $\langle h \rangle$ —mean wave thickness, h_{\max} , h_{\min} —maximum and minimum values of thickness [the scale of thickness is $h_s = (3\nu^2 Re/g)^{1/3}$], and c -phase velocity (the scale is equal to $\nu Re/h_s$) on the values of dimensionless wave numbers α [the scale is $(9Re^5/Fi)^{1/6}/h_s$] for the fall-down of the outer cylinder wall (wire) and inner cylinder wall (tube). Here, the values of Re and Fi numbers are fixed: $Re=4$, $Fi^{1/11}=6.8$ (water-glycerin-alcohol film). Both lines 1–4 and lines 1b–4b in Figures 6 and 7 correspond to the values of cylinder radius $R^{-1}=0, 0.05, 0.1$ and 0.2 , respectively.

Line 1 in Figure 6 corresponds to the case of a vertical plane. For this case, the solutions stem from the trivial solution $h=1$ at point $\alpha=1$, which on entering the linear instability region transform into a succession of solitary waves, $\alpha \rightarrow 0$. Up to the

value $\alpha \approx 0.55$, the wave profile is sine-like. Figure 8 compares out characteristic wave profiles and Nakoryakov et al.'s (1981) experiment (the dashed line), where $Re=7.2$ and $Fi^{1/11}=4.87$. In Figure 8a $\alpha \approx 0.531718$ (it corresponds to $\lambda=10.8$ mm in experimental profile), while in Figure 8b $\alpha=0.2$. Wave profiles represent two periods in ξ -direction. This comparison with experiment and more detailed ones by Trifonov and Tselodub (1991) demonstrates that waves close to sine waves observed in the experiments ("periodical" regimes) correspond quantitatively to some waves of this one-parameter family (henceforth the first family). The long waves of this family have a shape different from those in the experiment and by Trifonov and Tselodub (1991). They are unstable with respect to infinitesimal disturbances.

Line 1b in Figure 6 corresponds to long waves solutions, which quantitatively resemble "solitary" waves in above-mentioned experiments. As shown by Tselodub and Trifonov

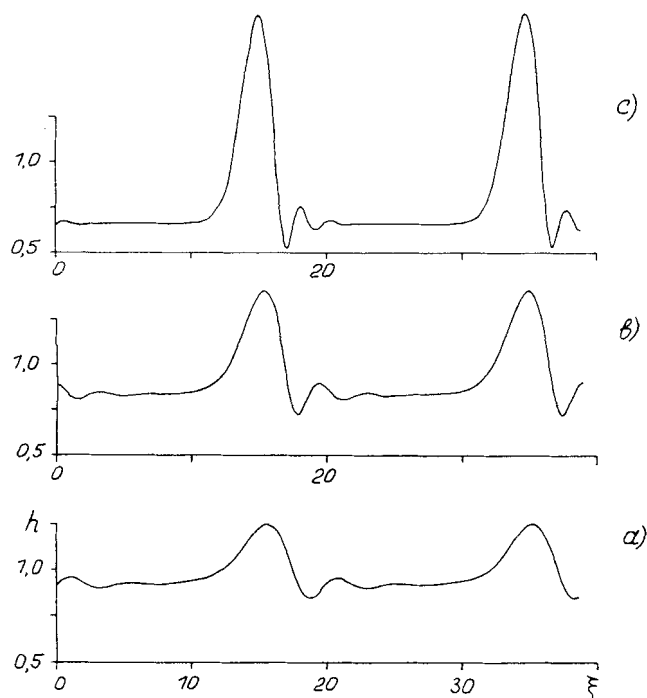


Figure 11. Characteristic waves with $\alpha = 0.32$.

The case of wire with $R^{-1} = 0$ (profile a); $R^{-1} = 0.1$ (b); $R^{-1} = 0.2$ (c).

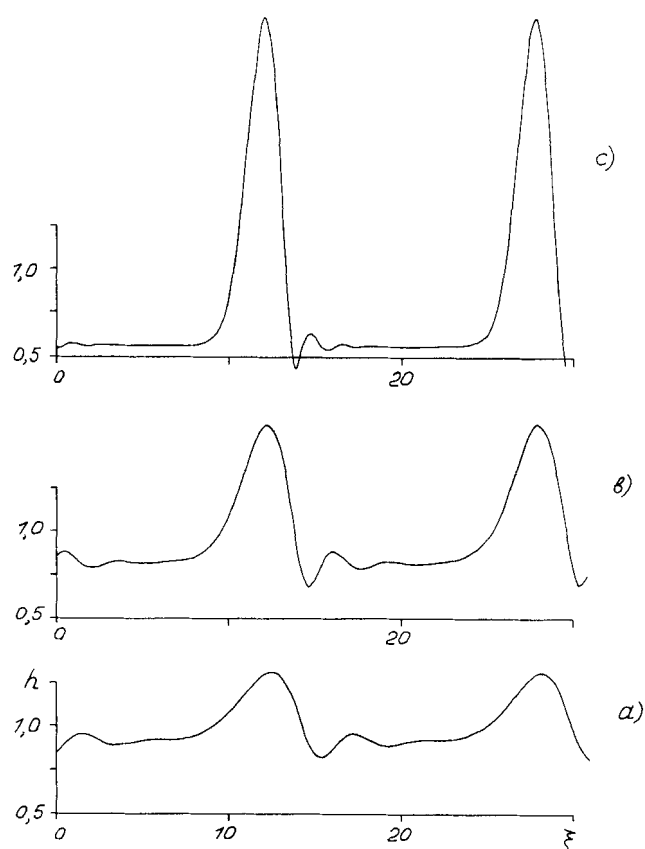


Figure 12. Characteristic waves with $\alpha = 0.4$.

The case of tube with $R^{-1} = 0.05$ (profile a); $R^{-1} = 0.1$ (b); $R^{-1} = 0.15$ (c).

(1991), this branch was generated from the corresponding wave of the first family with the double spatial period. Figure 9 compares the characteristic profiles of this second one-parameter family waves with Nakoryakov et al.'s experiment (1981) (the dashed line), where $Re = 7.2$ and $Fi^{1/11} = 4.87$. In Figure 9a $\alpha = 0.45$, while in Figure 9b $\alpha = 0.3$ and Figure 9c $\alpha \approx 0.16742$ (it corresponds to $\lambda = 34.3$ mm in experimental profile).

The case of a vertical plane was previously studied in detail by Trifonov and Tsvelodub (1985, 1988, 1991) and Demekhin and Shkadov (1985, 1989). Various steady-state traveling waves were calculated, and their stability and bifurcations were analyzed. They compared in detail the numerically obtained waves phase velocities, amplitudes and wave numbers with the correlations measured experimentally. It was demonstrated that the integral approximation provided a good quantitative description of large-amplitude waves observed in experiments. Here, the results of a vertical plane are compared with the case $R^{-1} \neq 0$, and the ability of integral approximation used is demonstrated. Unfortunately, no literature is available where the basic characteristics of waves of the surface of a film falling down on a vertical cylinder of radius comparable to film thickness were measured simultaneously. Therefore, we need to restrict the comparison with experiment to the case of a vertical plane.

In the case of falling down on the outer surface of a cylinder with finite radius, there are some qualitative conformities and differences with respect to the case of a vertical plane. Analogous to the case of a vertical plane, there are two branches of solutions: the limit of which at $\alpha \rightarrow 0$ is the "negative" solitary wave (the value $|h_{\max} - \langle h \rangle| < |h_{\min} - \langle h \rangle|$ and the shape of profile thickness is like the one in Figure 8b); the "positive" solitary wave (the value $|h_{\max} - \langle h \rangle| > |h_{\min} - \langle h \rangle|$ and the shape of profile thickness is like the one in

Figure 9c). One branch generates from the trivial solution (lines 2–4 in Figure 6), and the second branch generates from the corresponding wave of the first branch with the doubling of spatial period (line 2b–4b in Figure 6). The asymptotic behavior of the dependence $\langle h \rangle$, h_{\max} , and c is essentially different for these branches for all values of parameter R . Thus, if the limit of one branch as $\alpha \rightarrow 0$ is the "positive" solitary wave (lines 1b, 2b, 3b and 4 in Figure 6), the values of h_{\max} and c increase with decreasing α ; if the limit of a branch as $\alpha \rightarrow 0$ is the "negative" solitary wave (lines 1, 2, 3 and 4b in Figure 6), the same quantities decrease with decreasing α . The asymptotic behavior of value h_{\min} with a decrease in α is practically the constant for all values of wire radius and for both branches.

In addition, for all values of the wire radius, the values of $\langle h \rangle$, h_{\max} , and c vary in a smaller range with a decrease in α for the solution branch with the "negative" solitary wave limit than for the family with the "positive" solitary wave limit.

There is one qualitative difference between the fall-down on the wire with small enough radius (line 4 in Figure 6) and the fall-down on the vertical plane. The branch with the "positive" solitary wave limit emanates from the trivial solution, unlike a vertical plane where such a branch originates from the corresponding nonlinear wave of the first family with the doubling of spatial period.

On the inner surface of a cylinder with finite radius, there are also some qualitative conformities, but the differences from the vertical plane are more catastrophic. For some values of

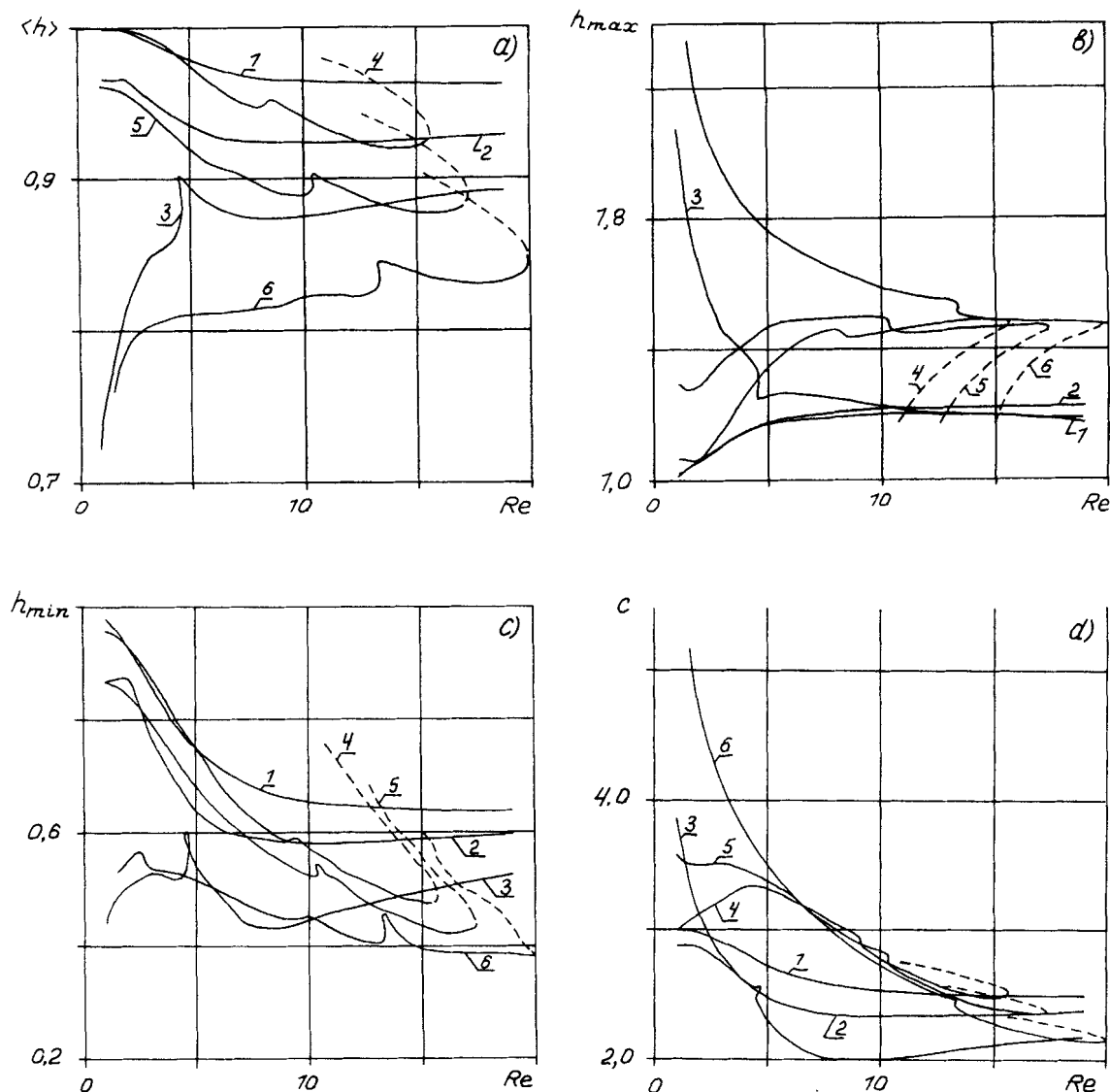


Figure 13. Characteristics of waves vs. Reynolds number at $Fi^{1/11} = 6.8$.

Lines 1–3, wave with $\alpha = 0.8$ branched from the trivial solution on the wires with $R^{-1} = 0.1$ and 0.2 , respectively; lines 4–6, $\alpha = 0.3$ (long wave) on the wires with the same values of radius.

parameter $R^{-1} < R_{cr}^{-1}(Re, Fi)$, there are two branches of solution: the limits of which when $\alpha \rightarrow 0$ are the “negative” solitary waves (lines 2, 3 and 4b in Figure 7) and the “positive” solitary wave (lines 2b and 3b) which is analogous to the vertical plane. Characteristic behavior of the $\langle h \rangle$, h_{max} , h_{min} , and c dependence for both branches is qualitatively identical to the fall-down of the outer surface of cylinder. For the values of parameter $R^{-1} > R_{cr}^{-1}$, the waves branching from the trivial solution (lines 4 in Figure 7) disappear for $\alpha < \alpha_{cr}$. The amplitude of solution quickly increases as one departs from the bifurcation point and the number of harmonics needed in series (8) increases drastically near the point α_{cr} . Further continuation along line 4 in Figure 7 was restricted by the computer abilities. The h_{max} value is close to the tube radius, and the h_{min} value is close enough to zero near the point α_{cr} .

From the results in Figures 6–9 we may conclude that there are at least two one-parameter branches of waves in the fall-down of the vertical cylinder. Comparison with experimental

results shows that the long waves, transformed into a series of “positive” solitary waves as $\alpha \rightarrow 0$, are realized in experiments. Therefore, we will consider only the corresponding branch of long waves.

Figures 10–12 show the dependence of the basic waves characteristics on the value of cylinder radius and some waves profiles, where the value of Reynolds number $Re = 4$ and that of film number $Fi^{1/11} = 6.8$. Lines 1 and 2 in Figure 10 correspond to the fall-down on the wire for the values of wave number $\alpha = 1.0$ (waves branched from the trivial solution) and $\alpha = 0.32$ (long waves), respectively. Some characteristic waves profiles ($\alpha = 0.32$) on two periods in ξ -direction are presented in Figure 11 for this case at $R^{-1} = 0.1$ and 0.2 , respectively. Lines 3 and 4 in Figure 10 correspond to the fall-down on the tube for the waves with $\alpha = 1.0$ and $\alpha = 0.4$, respectively. The profiles of waves with $\alpha = 0.4$ are presented in Figure 12 for $R^{-1} = 0.05, 0.1$ and 0.15 , respectively.

Figures 10–12 show that the wavy processes are increased

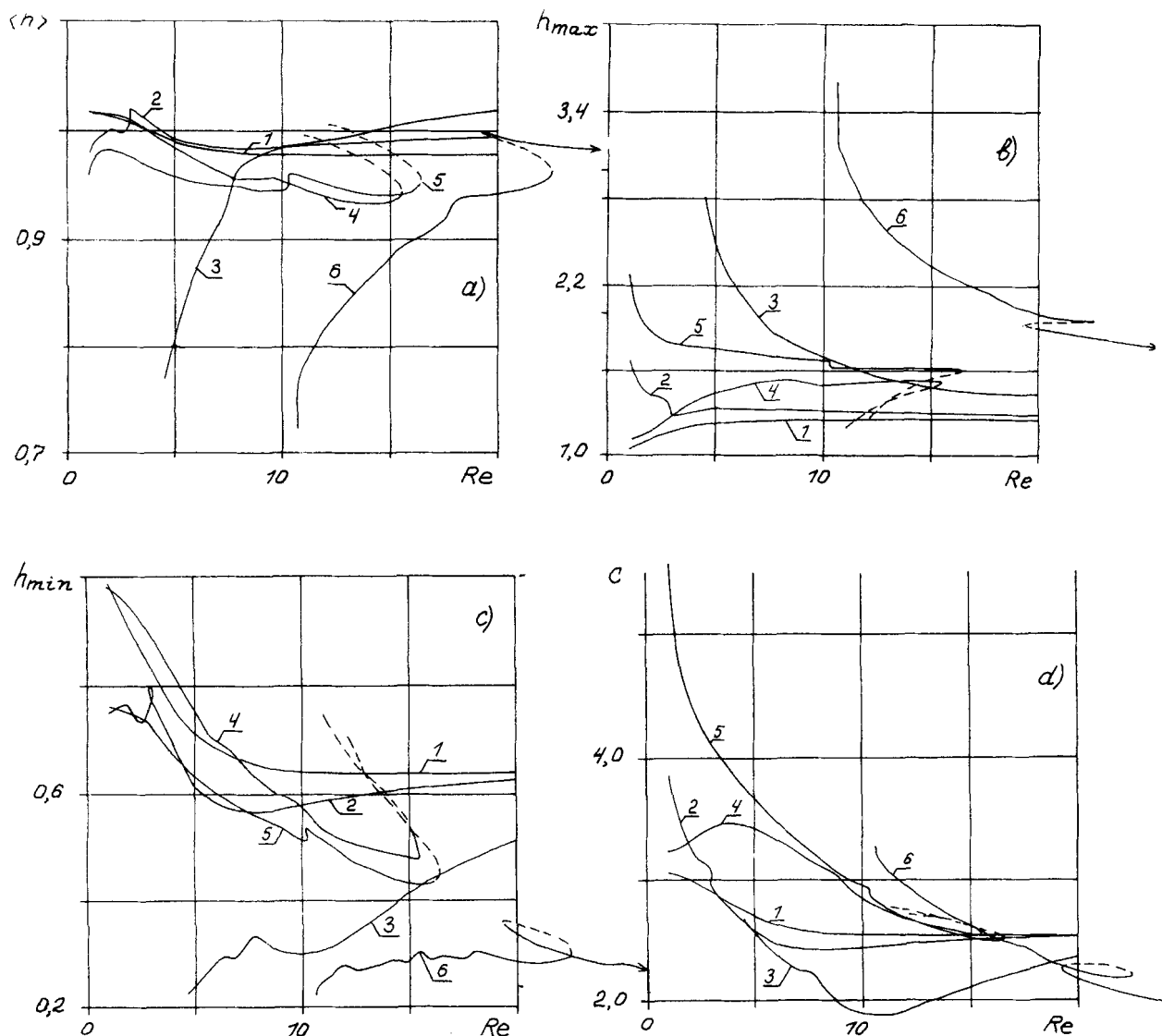


Figure 14. Characteristics of waves vs. Reynolds number at $Fi^{1/11} = 6.8$.

Lines 1-3, wave with $\alpha = 0.8$ branched from the trivial solution on the tubes with $R^{-1} = 0.05, 0.1$ and 0.2 , respectively; lines 4-6, $\alpha = 0.3$ (long wave) on the tubes with the same values of radius.

with decreasing cylinder radius. In the fall-down of the tube (lines 3 and 4 in Figure 10), there is a critical value Re_c that gives rise to catastrophic growth of the wave amplitude.

In Figures 13 and 14, the dependence of the basic waves characteristics on the value of Reynolds number is presented. Here, the value of film number $Fi^{1/11} = 6.8$ and the lines in Figure 13 correspond to the case of fall-down on the wire and the ones in Figure 14 for the case of falling down of the tube. Lines 1-3 in Figure 13 correspond to the characteristics of waves with wave number $\alpha = 0.8$ (waves branched from the trivial solution) at $R^{-1} = 0, 0.1$ and 0.2 , respectively. Lines 4-6 in Figure 13 correspond to the waves with $\alpha = 0.3$ (long waves) at the same values of wire radius. Lines 1-6 in Figure 14 correspond to the characteristics of waves with the same values of wave number as those of lines 1-6 in Figure 13 and at the same values of cylinder radius except for lines 1 and 4, which correspond to the case of fall-down of the tube with $R^{-1} = 0.05$.

There are some unique characteristics to the long waves,

lines 4-6 in Figures 13 and 14. The calculations show the existence of the turning points $Re_c(R^{-1})$ (dependence shown in Figures 13 and 14 are continued by the dashed lines after these points) such that the waves regimes corresponding to the cases 4-6 in Figure 13 and 4 and 5 in Figure 14 transform into the first-family solutions of the triple period in ξ -direction at the end of corresponding lines in Figures 13 and 14. In case 6 of Figure 14, there is a second turning point, and the dependence continues in the region of large Reynolds numbers. The calculations of the long waves characteristics on Reynolds number at the other values of parameter α show the existence of turning points for each value of α . For a given value of parameter R^{-1} , the turning points form a few loci $Re_c(\alpha)$. For various values of parameter α after returning from the corresponding lines, the waves may degenerate into the first-family waves with double, triple and so on period in the ξ -direction. It is difficult to calculate the loci of turning points for a wide range of parameters Re and α , and for a few values of pa-

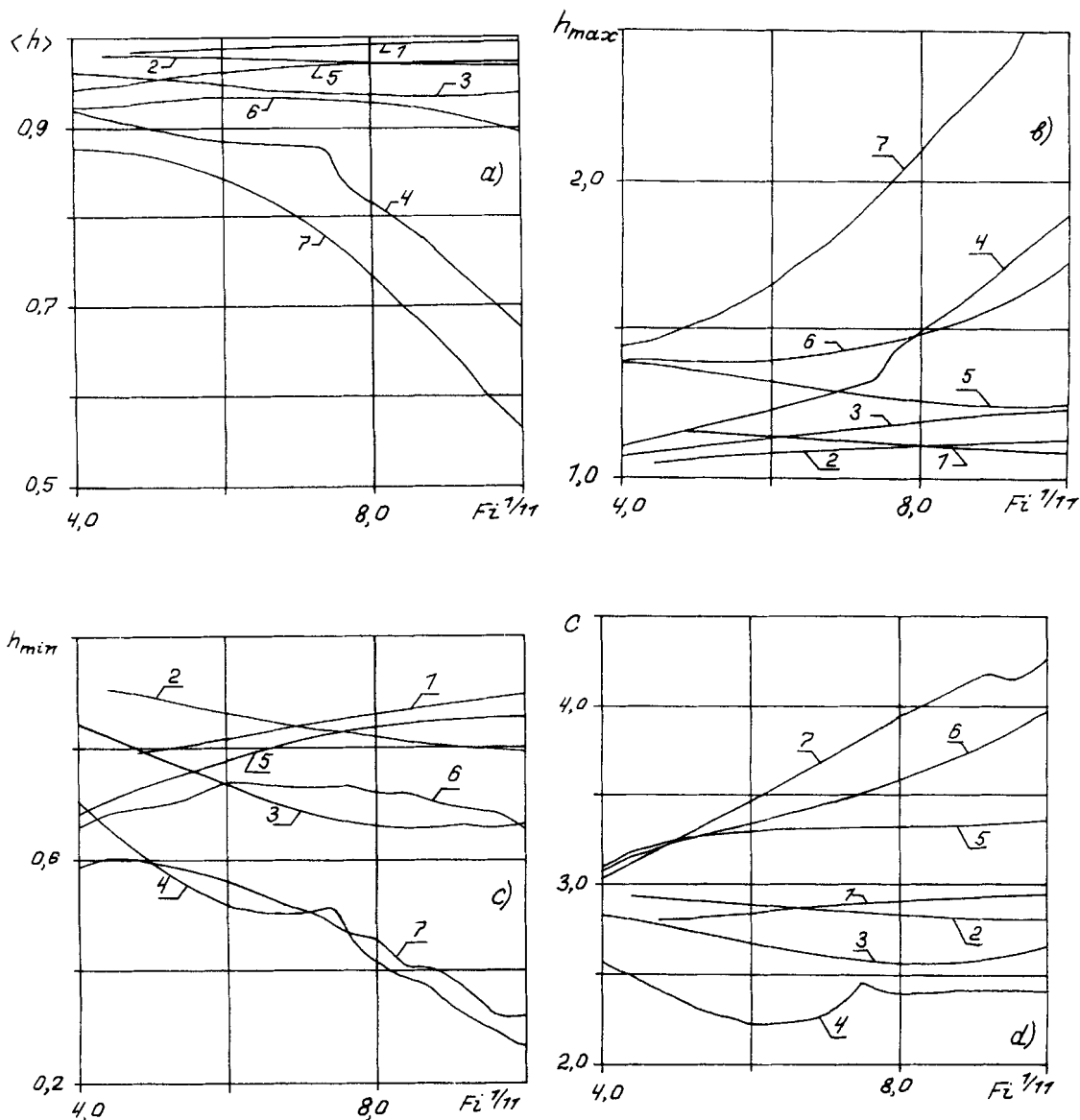


Figure 15. Characteristics of waves vs. film number at $Re=4$.

Line 1, wave with $\alpha=0.9$ at $R^{-1}=0$; lines 2-4, $\alpha=1.0$ wires with $R^{-1}=0.05, 0.1$ and 0.2 , respectively; lines 5-7, $\alpha=0.32$ (long wave) on the wires with $R^{-1}=0.05, 0.1$ and 0.2 , respectively.

parameter R^{-1} , and thus it is not carried out here. In the fall-down of the vertical plane, the loci used are by Tselodub and Trifonov (1991).

For a sufficiently small value of parameter R^{-1} (lines 1, 2, 4 and 5 of Figure 13; lines 1 and 4 of Figure 14), an increase in Reynolds number causes the increase in the wave intensity, as shown in Figures 13 and 14 (the waves on the dashed returning parts of the corresponding curves are not considered, because they are probably unstable). For the values of parameter R^{-1} corresponding to the lines 3 and 6 of Figure 13 and lines 2, 3, 5 and 6 of Figure 14, an increase in the Reynolds number causes the decrease in waves amplitudes. As shown in Figure 14, there is the critical growth of waves amplitudes at some values of parameters R^{-1} with the decrease in the Reynolds number in the fall-down of the tube.

In Figures 15 and 16, the dependence of the basic waves

characteristics on the value of film number is presented. Here, the value of the Reynolds number $Re=4$ and the lines in Figure 15 correspond to the case of the wire and ones in Figure 16 for the case of the tube. Line 1 in Figure 15 corresponds to the waves with the wave number $\alpha=0.9$ at $R^{-1}=0$ and lines 2-4 in Figure 15 waves with $\alpha=1.0$ at $R^{-1}=0.05, 0.1$ and 0.2 , respectively. Lines 5-7 in Figure 15 correspond to waves with the wave number $\alpha=0.32$ (the long waves) at $R^{-1}=0.05, 0.1$ and 0.2 . Lines 1-3 in Figure 16 correspond to waves with $\alpha=1.0$ at $R^{-1}=0.05, 0.1$ and 0.2 , and lines 4-5 in Figure 16 waves with $\alpha=0.4$ at the values of $R^{-1}=0.05$ and 0.1 , respectively.

Figures 15 and 16 show that at some small values of parameter R^{-1} (lines 1 and 5 in Figure 15; line 4 in Figure 16), an increase in the film number causes the decrease in the waves intensity. At the great enough values of R^{-1} , the increasing film number results in the destabilizing effect.

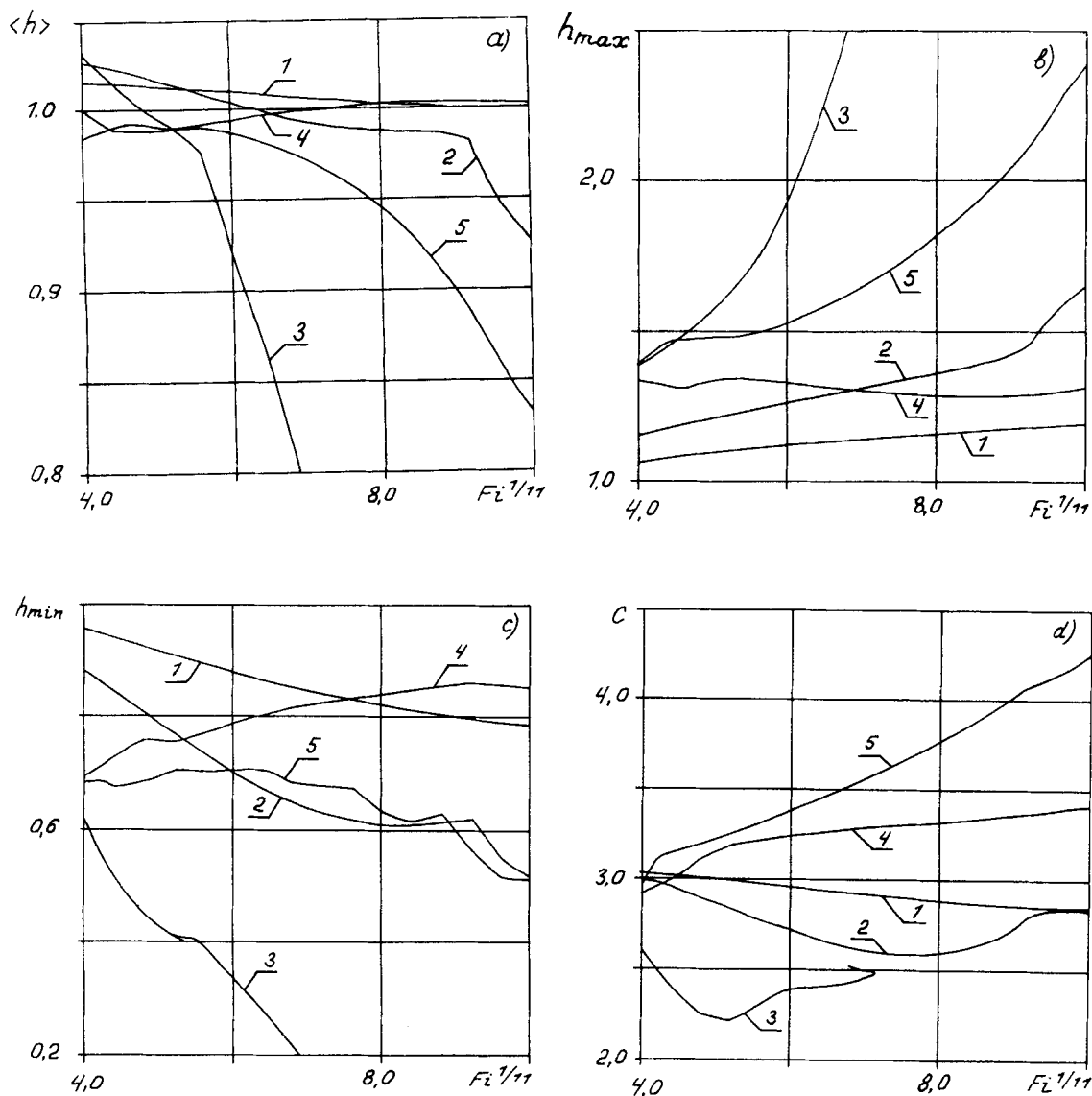


Figure 16. Characteristics of waves vs. film number at $Re=4$.

Lines 1–3, wave with $\alpha=1.0$ on the tubes with $R^{-1}=0.05, 0.1$ and 0.2 , respectively; lines 4–5, $\alpha=0.4$ (long wave) on the tubes with $R^{-1}=0.05$ and 0.1 , respectively.

Conclusions

Various nonlinear wavy regimes of a thin viscous liquid layer flowing down the outer and inner surfaces of a vertical cylinder were considered. By using an integral method, a system of equations was obtained to describe the evolution of long-wave disturbances. There are three external parameters (Reynolds number Re , film number Fi , and the wall curvature R^{-1}) in this model. The linear stability analysis of flowing with the smooth free surface was investigated, and the results agreed with those by other authors, who used expansion of the Navier-Stokes equations solutions in powers of the small long-wave parameter. The smooth free surface is unstable at any value of external parameters. The disturbances evolution are ruled by gravitational force (the pumping of energy), viscous forces (the damping of energy), and forces of the surface tension. The calculations show that the wall curvature has a destabilizing effect. This differs from the capillary forces related to

the film thickness variation, since capillary forces associated with the wall curvature try to increase the elevation of the film thickness from the mean level. As a consequence, the decrease in the cylinder radius promotes the waves formation process.

As a result of the evolution, steady traveling solutions may be formed, as the calculations proved. The main concern was with the qualitative differences and conformities of the wave characteristics in the fall-down on the inner or outer cylinder surfaces from the wave characteristics in the fall-down on a vertical plane. The calculations show that both in the fall-down on the wires and of a vertical plane, there are at least two waves families parameterized by the wave number at the fixed values of external parameters. Waves of these families transform either into the succession of “negative” solitary waves as $\alpha \rightarrow 0$ or into the succession of “positive” solitary waves. In the case of fall-down on the inner surface of a vertical cylinder, the family with the “negative” solitary wave limit as

$\alpha \rightarrow 0$ exists at all values of external parameters, but the family with the "positive" solitary wave limit exists only for small wall curvature. Catastrophic growth of the amplitude of steady traveling waves occurs in the film fall-down on a vertical tube away from the neutral curve of smooth solution.

In comparison with the case of falling down on a vertical plane, the external parameters Re and $Fi^{1/11}$ have different influence. Thus, in the case of falling down of a vertical plane, an increase in the Reynolds number Re causes the wavy processes intensity to increase and that in film number causes the decrease in the wave intensity. In the case of falling-down of the wires or tubes with small radius increasing Reynolds number causes the decrease in the wave intensity due to a decrease in the relative curvature. The increase in the film number is accompanied by both stabilizing and destabilizing effects of capillary forces. As a result, an increase in the film number causes a decrease in the wave intensity in the case of a vertical cylinder with small radius.

Notation

- c = phase velocity (for infinitesimal disturbance it is a complex value; for nonlinear regime, real)
 c_2 = dimensionless phase velocity = c/u_{\max}
 f, f_1 = special functions
 Fi = film number = $(\sigma/\rho)^{3/4} g \nu^4$
 g = gravitational acceleration
 h_o = dimensional mean film thickness
 h = film thickness
 h_{\max}, h_{\min} = maximum and minimum values of thickness
 h_N, q_N = dimensional film thickness and flow rate of the smooth flow
 h^*, h_s = scales of the smooth and wavy film thickness = $(3\nu q_N/g)^{1/3}, (3\nu q_o/g)^{1/3}$
 $\langle h \rangle$ = mean film thickness = $(1/\lambda) \cdot \int_0^\lambda h(\xi) d\xi$
 H_k = Fourier harmonic
 L = scale in the z -direction
 P, P_o = pressure, atmospheric pressure
 q_o = dimensional mean flow rate
 r = radial distance from the wire (tube) axis
 R^{-1} = curvature of wall
 R_2 = dimensionless radius = R/h_N
 Re = Reynolds number = q_o/ν
 Re_1 = Reynolds number = $u_o h_o/\nu$
 Re_2 = Reynolds number = $u_{\max} h_N/\nu$
 t = time
 u_o = scale of velocity in the z -direction = $gh_o^2/3\nu$
 u = velocity in the z -direction
 u_{\max} = velocity on the free film surface
 v = velocity in the r -direction
 We = Weber number = $(3Fi/Re^5)^{1/3}$
 We_2 = Weber number = $(\sigma/\rho)/gh_N^2$
 y = special variable = $1 \pm h(z, t)/R$
 z = axial distance

Greek letters

- α = wave number = $2\pi/\lambda$
 δ = distance from the wall
 ϵ = small parameter = h_o/L
 λ = wave length
 μ = dimensionless wave number = $2\pi h_N/\lambda$
 ν = kinematic viscosity
 ρ = density
 σ = surface tension
 ξ = $z - ct$

Upper signs

- * = dimensionless variables
 ' = infinitesimal disturbances

Literature Cited

- Alekseenko, S. V., V. Ye. Nakoryakov, and B. G. Pokusaev, "Wave Formation on a Vertical Falling Liquid Film," *AIChE J.*, **31**, 1446 (1985).
 Bach, P., and J. Villadsen, "Simulation of the Vertical Flow of a Thin Wavy Film Using a Finite-Elements Method," *Int. J. Heat and Mass Transfer*, **27**, 815 (1984).
 Benjamin, G. B., "Wave Formation in Laminar Flow Down on Inclined Plane," *J. Fluid Mech.*, **2**, 554 (1957).
 Benney, D. J., "Long Waves in Liquid Film," *J. Math. Phys.*, **45**, 150 (1966).
 Demekhin, Ye. A., and M. A. Kaplan, "Stability of Stationary Traveling Waves on the Surface of a Vertical Film of Viscous Fluid," *Izv. Akad. Nauk. SSSR, Ser. Mekh. Zhidk. i Gasa*, **3**, 33 (1989).
 Demekhin, Ye. A., and V. Ya. Shkadov, "Two-Dimensional Wave Regimes of a Thin Viscous Film," *Izv. Akad. Nauk. SSSR, Ser. Mekh. Zhidk. i Gasa*, **3**, 63 (1985).
 Demekhin, Ye. A., M. A. Kaplan, and R. A. Foigel, "Nonlinear Waves in a Flowing Viscous Layer of a Magnetic Liquid," *Magnitn. Gidrodynamika, SSSR*, **1**, 21 (1988).
 Gjevik, B., "Occurrence of Finite-Amplitude Surface Waves on Falling Liquid Films," *Phys. Fluids*, **13**(8), 1918 (1970).
 Goren, S. L., "The Instability of an Annular Thread of Fluid," *J. Fluid Mech.*, **12**, 309 (1962).
 Kapitza, P. L., and S. P. Kapitza, "Wave Flow of Thin Viscous Liquid Films," *Zh. Teor. Fiz.*, **19**, 105 (1949).
 Lin, S. P., "Finite-Amplitude Stability of a Parallel Flow with a Free Surface," *J. Fluid Mech.*, **36**, 113 (1969).
 Lin, S. P., and W. C. Liu, "Instability of Film Coating of Wires and Tubes," *AIChE J.*, **21**(4), 775 (1975).
 Nakaya, C., "Long-Waves on a Thin Fluid Layer Flowing Down an Inclined Plane," *Phys. of Fluids*, **18**, 1407 (1975).
 Nakoryakov, V. E., et al., "Instantaneous Velocity Profiles in a Wave Liquid Film," *Inzh. Fiz. J., SSSR*, **33**, 399 (1977).
 Nakoryakov, V. E., B. G. Pokusaev, and S. V. Alekseenko, "Desorption of Weakly-Solution Gas from Flowing Liquid Films," *Calculation of Heat and Mass Transfer in Energy-Chemical Processes*, A. P. Burdukov, ed., Institute of Thermophysics, Novosibirsk, 23 (1981).
 Nepomnyashchy, A. A., "Wave Regime Stability in a Film Falling Down Inclined Surfaces," *Izv. Akad. Nauk. SSSR, Ser. Mekh. Zhidk. i Gasa*, **3**, 28 (1974).
 Shkadov, V. Ya., "Wave Modes in the Gravity Flow of a Thin Layer of a Viscous Fluid," *Izv. Akad. Nauk. SSSR, Ser. Mekh. Zhidk. i Gasa*, **1**, 43 (1967).
 Shlang, T., and G. I. Sivashinsky, "Irregular Flow of a Liquid Film Down a Vertical Column," *J. Physique*, **43**, 459 (1982).
 Tougou, H., "Long Waves on a Film Flow of a Viscous Fluid Down the Surface of a Vertical Cylinder," *J. Phys. Soc. Japan*, **43**(1), 318 (1977).
 Trifonov, Yu. Ya., and O. Yu. Tselodub, "Nonlinear Waves on the Surface of a Liquid Film Falling Down a Vertical Plane," *Prikl. Mekh. i Tekhn. Fiz., SSSR*, **5**, 15 (1985).
 Trifonov, Yu. Ya., and O. Yu. Tselodub, "Stationary Two-Dimensional Waves on a Vertically Falling Down Liquid Film and Their Stability," *Inzh. Fiz. J., SSSR*, **54**, 1 (1988).
 Trifonov, Yu. Ya., and O. Yu. Tselodub, "On Branching of Steady-State Traveling Wavy Regimes of a Viscous Liquid Film," *Prikl. Mekh. i Tekhn. Fiz., SSSR*, **4**, 55 (1988).
 Trifonov, Yu. Ya., and O. Yu. Tselodub, "Nonlinear Waves on the Surface of a Falling Down Liquid Film: 1. Waves of First Family and Its Stability," *J. Fluid Mech.*, **229**, 531 (1991).
 Tselodub, O. Yu., and Yu. Ya. Trifonov, "Nonlinear Waves on the Surface of a Falling Down Liquid Film: 2. Bifurcations of the First-Family Waves and the Others Types of Nonlinear Waves," *J. Fluid Mech.*, in press (1992).
 Yih, Ch.-S., "Stability of Liquid Flow Down on Inclined Plane," *Phys. Fluids*, **6**, 321 (1963).

Manuscript received July 1, 1991, and revision received Nov. 18, 1991.